Electrostatic Tuning of Ion Conductance in Potassium Channels

Crina M. Nimigean, Joshua S. Chappie, and Christopher Miller*

Department of Biochemistry, Howard Hughes Medical Institute, Brandeis University, Waltham, Massachusetts 02454

Received May 23, 2003; Revised Manuscript Received June 24, 2003

ABSTRACT: Members of the K^+ channel family display remarkable conservation of sequence and structure of the ion selectivity filter, whereas the rates of K^+ turnover vary widely within the family. Here we show that channel conductance is strongly influenced by charge at the channel's intracellular mouth. Introduction of a ring of negative charges at this position in KcsA, a bacterial K^+ channel, augments the conductance in a pH-dependent manner. These results are explained by a simple electrostatic effect based on known channel structures, where the negative charges serve to alter the electrical potential at the inner mouth and, thus, to increase the local K^+ concentration. In addition, removal of the conserved negative charges at equivalent positions in a high-conductance eukaryotic K^+ channel leads to a decrease in conductance.

K^+ channels form a ubiquitous molecular family of membrane proteins whose common purpose is to provide transmembrane ionic diffusion pathways specific for K^+ ions. They are activated by many different kinds of cellular signals, as is reflected in the numerous classes and subclasses of K^+ channel sequences found in virtually all genomes. But within this variety there exists a striking unity: common sequences forming identical pore structures where discrimination for K^+ ions occurs (*1*−*4*). In light of the strong conservation of sequence and structure among K^+ selectivity filters, as well as their nearly identical ion-selectivity properties, it is perplexing that K^+ channels display a broad span of absolute rates of K^+ permeation. Most of the intensely studied types of eukaryotic K^+ channels show single-channel conductances encompassing values of roughly 5−50 pS at physiological concentrations of K^+ (*5*). Standing out from these, the "BK" class of Ca^{2+}-activated K^+ channels shows unusually high conductance of 200−300 pS, representing ion transport rates of $\sim 10^8$ ions/s (*6*). By engineering the single-channel properties of KcsA, a bacterial K^+ channel, we show that a significant part of this difference may be quantitatively understood in terms of the distribution of charges on the cytoplasmic vestibule leading up to the selectivity filter.

METHODS

Channel Expression and Generation of Mutant Channels. Mutant channel subunits (A108D, A108E, A108N, and A108Q for KcsA, E321N/E324N for BK) were constructed using standard mutagenesis methods. (Single neutral mutants of the BK channels were not analyzed because they were both close in conductance to wild type.) N-Terminal His-labeled KcsA wild-type and mutant channels were overexpressed in *Escherichia coli* (JM-83) and purified over a Ni-NTA agarose column as described (*7*). Purified channel protein was reconstituted into liposomes as described (*8*) . The BK channel wild-type [mSlo, L16912 in the mBR5 construct (*9*)] and mutant clones were in vitro transcribed using standard procedures, and 0.5−50 ng of cRNA was injected into *Xenopus laevis* oocytes for single-channel recording 2−8 days later. The functional integrity of the mutated channels was confirmed by the preservation of basic elements of single-channel personality such as bursting kinetics, pH or Ca^{2+} dependence, open-channel $I-V$ curves, selectivity, and Ba^{2+} block. We also attempted to record KcsA-A108R channels but failed in these attempts.

Single-Channel Recordings and Analysis. Liposome-reconstituted KcsA was incorporated into planar lipid bilayers as described (*10*). Single-channel recordings were taken in symmetrical 100 mM K^+ solutions (85 mM KCl, 15 mM KOH) buffered with 5 mM Mops and 5 mM succinic acid and adjusted with HCl to pH 7.0 and 3.0−6.0 for the external and internal solutions, respectively. BK channels were recorded using inside-out patches pulled from oocytes in 100 mM symmetrical K^+ (80 mM potassium gluconate, 5 mM KCl, 15 mM KOH, 5 mM Mops, and 5 mM succinic acid, adjusted to pH 7.0 with HCl) and 3−10 μM internal Ca^{2+} and external 2 mM Mg^{2+}; for oocytes expressing many channels per patch, 10 μM internal Ba^{2+} was included to favor the observation of single opening events; though BK expression levels were variable, similar results were obtained from high- and low-expressing oocytes. Recordings were collected with an Axopatch 200 amplifier, sampled at 10−50 kHz, and low-pass filtered at 2−5 kHz. Occasionally, small amplitude currents recorded at low voltage values were digitally filtered offline at 0.25−1 kHz. Conductances for BK were measured at 100 mV.

Modeling. An electrostatic treatment based on MthK as a model for the open state of KcsA was used to calculate the pH dependence of conductance expected for KcsA-A108D from Scheme 1. Assuming that protonation is fast compared

* To whom correspondence should be addressed. E-mail: cmiller@brandeis.edu. Phone: 781-736-2340. Fax: 781-736-2365.

10.1021/bi0348720 CCC: $25.00
Published on Web 07/18/2003

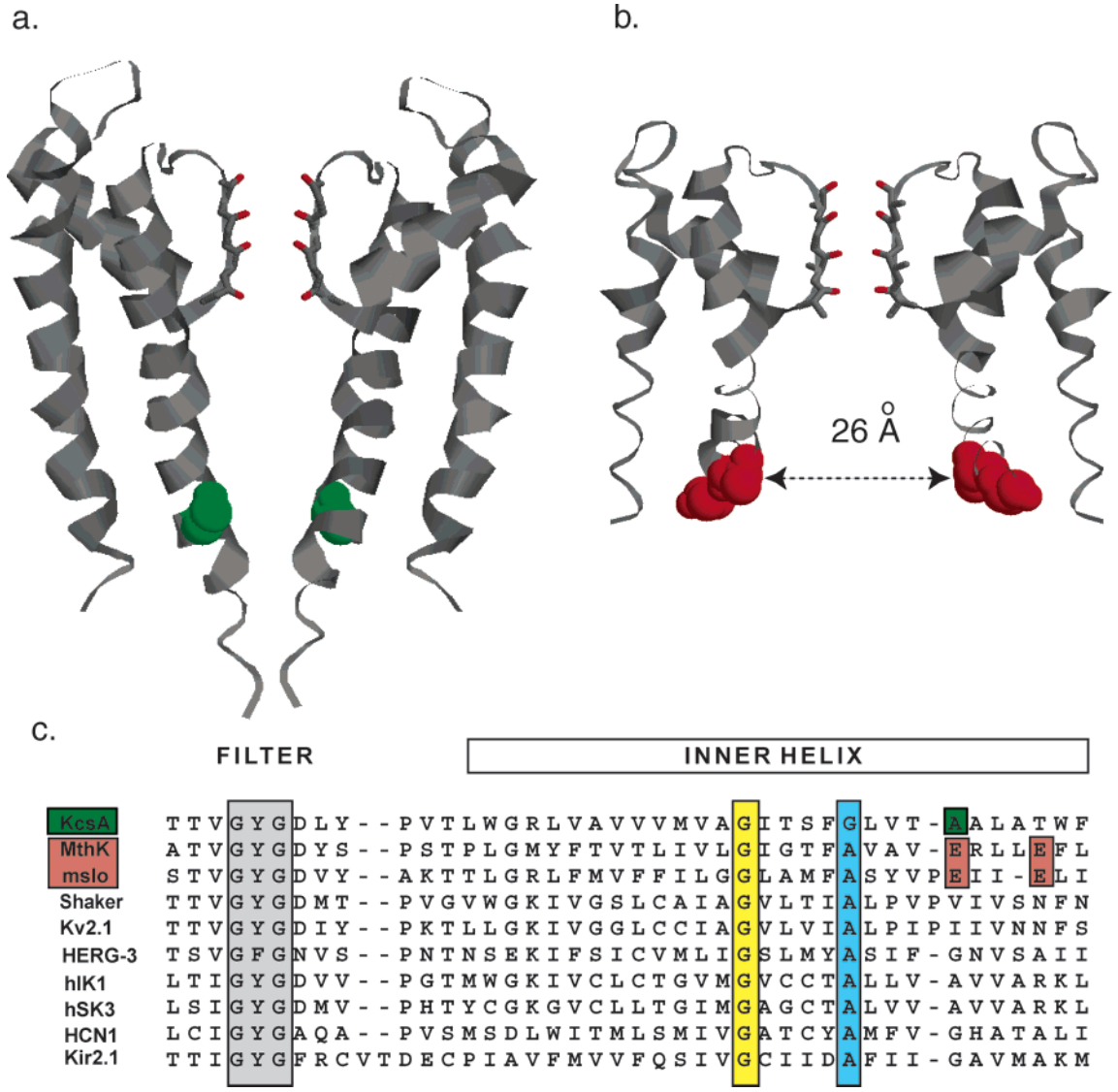

FIGURE 1: Representations of the structure and primary sequence of K^+ channel pores. Two opposing subunits of the tetrameric channels are shown for KcsA (*2*) (a) or MthK (*3*) (b). Residues A108 in KcsA and E92 and E96 in MthK are space-filled and highlighted in green and red, respectively. (c) Alignment of the K channel pore region, emphasizing the selectivity filter (gray), inner helix (white), hinge glycine (yellow), and bundle crossing (cyan). Positions of residues examined here are also indicated: MthK E92, E96 and BK E321, E324 (red); KcsA A108 (green).

to the time resolution of the recording system, the observed conductance, $\langle\gamma\rangle$, is a time average:

$$\langle\gamma\rangle = \sum f_j\gamma_j \tag{1}$$

where f_j is the pH-dependent probability of the jth form, γ_j is the pH-independent conductance of that form, and the sum is over all six forms of the channel. In addition, the variation of wild-type channel conductance with bulk K^+ concentration, $\gamma_{wt}([K^+]_b)$ is known (*7*) and is related to the local K^+ concentration under the influence of electrostatic potential by

$$\gamma_j = \gamma_{wt}([K^+]_b e^{-\psi_j}) \tag{2}$$

where ψ_j is the normalized potential (with j protons bound) at a position on the channel axis at the level of the aspartate substitutions. By assumption 3 in the text:

$$\psi_j = \frac{q_e F}{4\pi\epsilon_0 DRTa}(4 - j) \tag{3}$$

where q_e is the electronic charge, a is the radial distance to the substituted charges (13 Å), D is the dielectric constant (78), and F, R, and T have their usual meanings. With these parameters, the dimensionless factor multiplying $(4 - j)$ in eq 3 becomes 0.54.

An empirical function describing the conductance of wild-type KcsA on bulk K^+ concentration was derived by fitting published data (*7*) to a double-rectangular hyperbola. The observed pH-dependent conductance was then calculated from eq 1 by using this function in eq 2. The pH-dependent probabilities, f_j, were calculated from an Adair binding scheme on chemically identical sites, constructing the binding

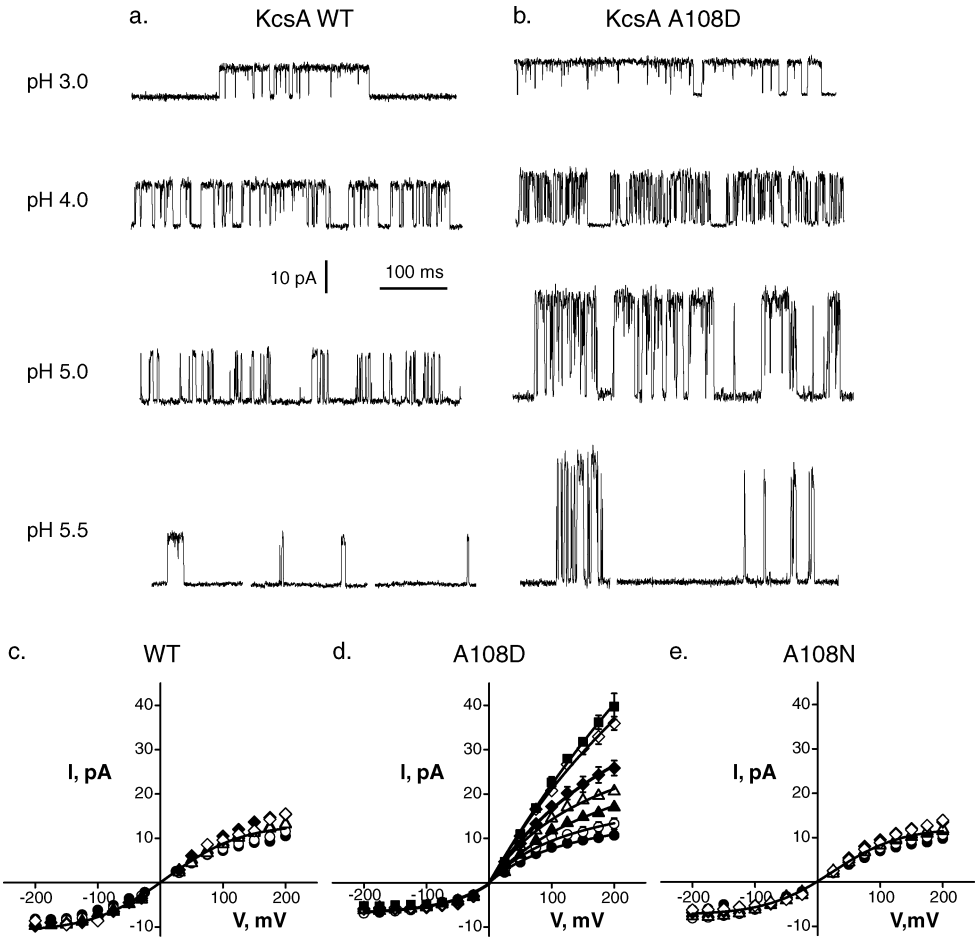

FIGURE 2: Currents through wild-type and mutant KcsA as a function of pH. Raw single-channel recordings (a, b) of wild-type KcsA and A108D KcsA are shown at the indicated pH values at 200 mV holding potential. $I-V$ curves of wild-type, A108D, and A108N are shown in panels c−e. Each data point represents the average ± SE from at least three separate bilayers. Symbols are as follows: filled circles, pH 3.0; empty circles, pH 3.5; filled triangles, pH 4.0; empty triangles, pH 4.5; filled diamonds, pH 5.0; empty diamonds, pH 5.5; filled squares, pH 6.0.

partition function with conventional statistical factors and electrostatic cooperativity factors appropriate to the geometry of the aspartate groups, as given by the MthK structure. According to this treatment, the stepwise macroscopic association constants, K_i, are given in terms of the intrinsic microscopic association constant k and the radial position, a, of the unprotonated aspartate groups:

$$K_1 = 4k \exp(({}^1/_2 + \sqrt{2})C/a)$$

$$K_{2d} = {}^1/_2 k \exp(\sqrt{2}C/a) \qquad \text{diagonal}$$

$$K_{2a} = 1k \exp([(1 + \sqrt{2})/2]C/a) \qquad \text{adjacent}$$

$$K_3 = 2k \exp({}^1/_2 C/a)$$

$$K_4 = {}^1/_4 k$$

where

$$C = \frac{q_e F}{4\pi\epsilon_0 DRT}$$

Accordingly, the proton-binding partition function, $Q(h)$, is

$$Q(h) = 1 + K_1 h + K_1(K_{2a} + K_{2d})h^2 + K_1(K_{2a} + K_{2d})K_3 h^3 + K_1(K_{2a} + K_{2d})K_3 K_4 h^4 \quad (4)$$

where h represents proton concentration.

RESULTS AND DISCUSSION

Figure 1 presents the crystal structures of the pore domains of two K^+ channels, KcsA and MthK, which have been proposed as general structural models for K^+ channel closed and open conformations, respectively (*2*, *3*, *11*). These channels may also be considered prokaryotic proxies for the two conductance types mentioned above; KcsA, with conductance of ~50 pS, falls into the major category of K^+ channels, while the MthK pore has a high, BK-like conductance of 200 pS. Since the identical selectivity-filter sequences of these two channels adopt virtually superimposable structures (*12*), we looked elsewhere for possible conductance determinants that might account for this difference. Sequence alignment of various K^+ channels in the pore-forming region (Figure 1c) reveals an obvious feature appearing exclusively in all BK-type channels, including MthK. These high-conductance channels uniquely have negatively charged residues in the inner helix at two positions 3−4 helical turns

Scheme 1

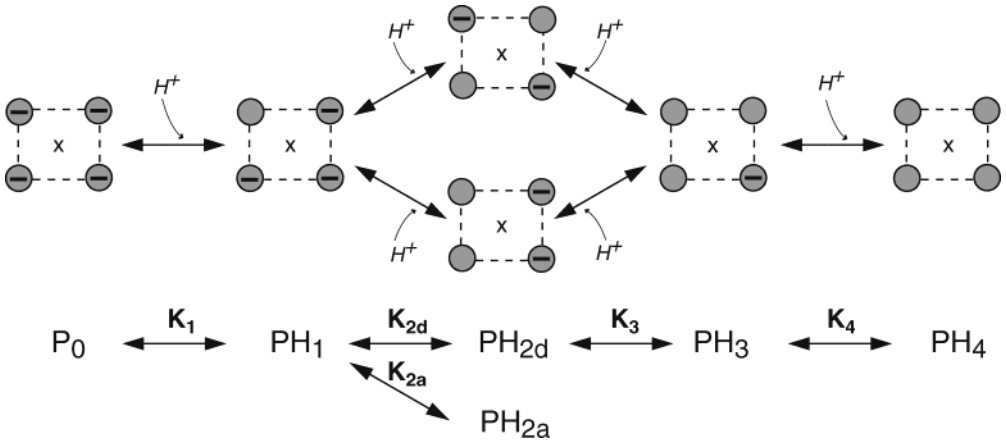

following the conserved "hinge" glycine (*3*). In the closed conformation, the first of these positions (A108 in KcsA) lies close to the "bundle crossing" that forms the intracellular gate (*2*, *13*), while in the open conformation, this position (E92 in MthK) swings out to the edge of the wide intracellular vestibule, where permeating ions depart the aqueous solution and formally enter the channel; the second glutamate (E96) of MthK is located closeby in space, one helical turn beyond this position. These structural characteristics suggest a simple mechanism for influencing absolute conductance by placing charged groups upon this crucial location near the ion entryway and thereby altering local K^+ concentration via through-space electrostatics.

This mechanism predicts that the single-channel conductance of KcsA should increase by substitution of negatively charged side chains at position 108. A complication in implementing this simple experiment, however, is that KcsA requires low pH (3−4) on the intracellular side for activity (*14*), and the channel open probability falls off drastically as the internal pH is raised toward neutrality. For this reason, we cannot simply compare wild-type and carboxyl-substituted channels at neutral pH, where the side chain would be fully deprotonated, but instead must examine single channels over a wide pH range. As illustrated in Figure 2, the amplitude of single-channel currents in wild-type KcsA is nearly insensitive to pH. The conductance of the aspartate mutant, A108D, is similar to that of wild type at pH 3, where the aspartyl side chain is electrically neutral. But as the pH is increased and the carboxyl group deprotonates, the A108D conductance increases dramatically to ∼200 pS, a value characteristic of BK channels. Substitutions at position 108 are known to increase this channel's open probability (*15*), and so it was possible to observe the mutant at pH as high as 6, where wild-type channels were never detected. The single-channel current−voltage (*I*−*V*) curves (Figure 2d) show a more pronounced pH effect at positive voltage, as expected from the intracellular position of the substituted charges. Substitution of asparagine, a neutral isostere, is pH-insensitive like wild type (Figure 2c,e). A similarly strong pH-dependent conductance increase also occurs in the A108E mutant but not in the A108Q neutral isostere (data not shown).

The fact that pH dependence is specifically conferred upon the channel conductance by carboxyl substitutions at position 108 argues that the effect is a direct reflection of a negative

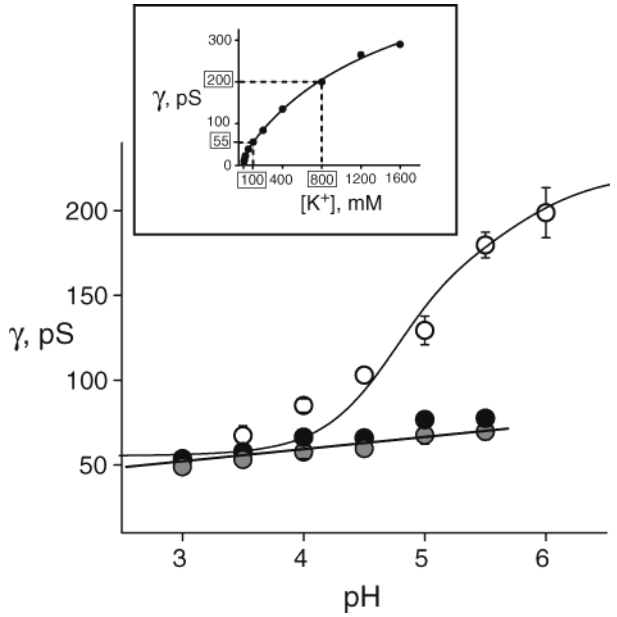

FIGURE 3: Residue 108 determines the pH sensitivity of KcsA conductance. Chord conductances at +200 mV (γ) were determined as a function of pH for wild-type (black filled circles), A108D (empty circles), and A108N (gray filled circles). The smooth curve is calculated from eqs 1−3, with $D = 78$, $a = 13$ Å, and $pK_a = 4.7$. Inset: conductance−concentration curve for wild-type KcsA (*7*). Dashed lines emphasize the 8-fold increase in local K^+ concentration (boxed values) due to the introduction of the four negatively charged residues, corresponding to high and low asymptotic conductance values from the calculated pH titration curve. Similar results were obtained using conductance at 100 mV.

electrostatic potential near the ion entryway growing as the side chains progressively deprotonate. We envision that the local K^+ concentration near the intracellular vestibule, and hence the conductance, responds to the potential emanating from the four aspartate residues on the homotetrameric channel, according to their average state of deprotonation. This picture may be quantified in a simple way, assuming (1) that the structure of MthK provides a valid model for the open conformation of KcsA, (2) that the local K^+ concentration sensed by the channel follows the electrostatic potential at the entry to the intracellular vestibule, and (3) that a summed Coulombic potential describes the influence of the four aspartate residues on each other and on local K^+ concentration at the vestibule entry. We consider a homotetrameric channel with six distinguishable states of protonation,

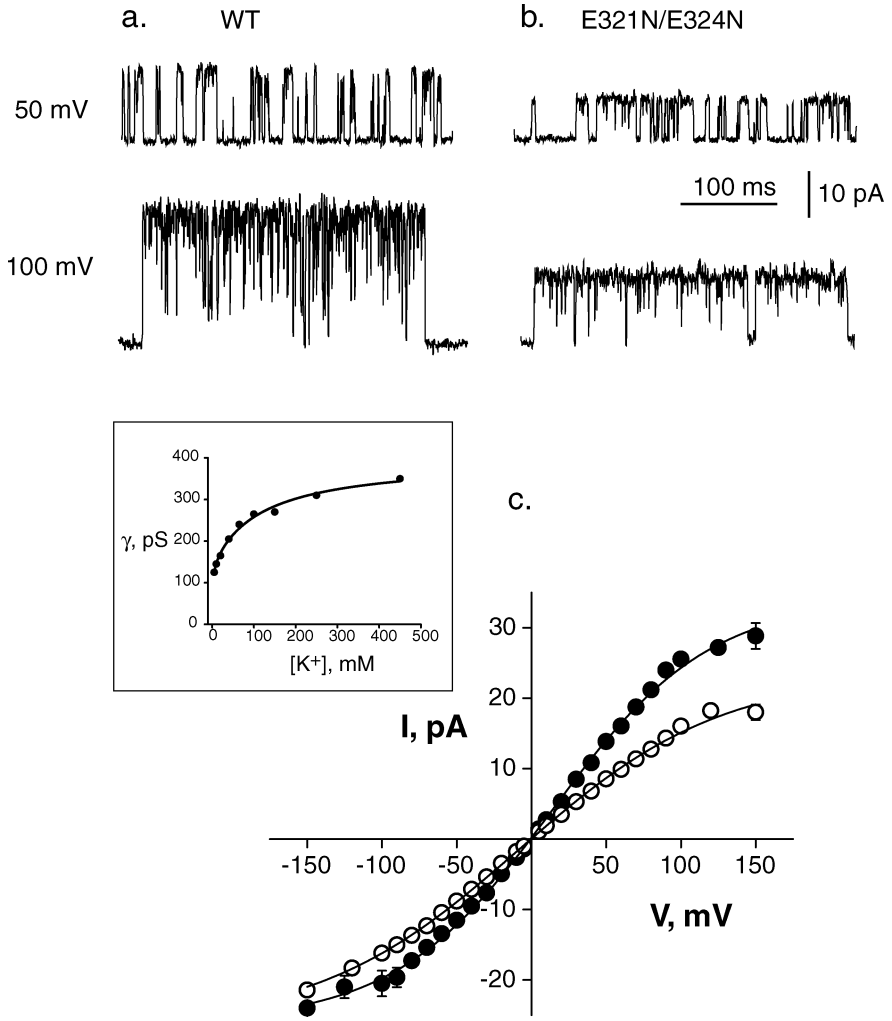

FIGURE 4: Neutralization of the two glutamate residues at the inner mouth of the BK channel induces a decrease in conductance. Single-channel currents through wild-type (a) and E321N/E324N (b) BK channels at +50 and +100 mV are shown, along with $I-V$ curves (c). Data points represent averages ± SE of 6 patches for wild-type BK (filled circles) and 16 patches for the E321N/E324N mutant (empty circles). The inset shows the conductance−concentration relationship for the rat skeletal muscle BK channel taken from ref *17*.

the numbers referring to protons bound, and each reaction representing a proton-binding step, according to Scheme 1. The scheme cartoons the various protonation states of the pertinent aspartate residues (upper panel) and presents the formal linked equilibria involved (lower panel).

The states labeled 2a and 2d represent forms with two protons bound in adjacent or diagonal configurations. To obtain the pH dependence of appearance of the various protonation forms, we treat proton binding by conventional linked-equilibrium methods (*16*), with each protonation step occurring under the electrostatic influence of the other deprotonated aspartates in the tetramer, as calculated from the structure of MthK; this produces a weak negative cooperativity in H^+ binding because the attractive electrostatic potential at each proton-binding site decreases with increasing site occupancy. Since protonation kinetics of a typical carboxyl group are much faster than our time resolution, the observed conductance is a time average of the pH-independent conductances of the individual forms in Scheme 1, weighted according to their pH-dependent probabilities.

Given these assumptions, along with the crystallographically determined 13 Å radial distance of the aspartates in the MthK vestibule (*12*), the pH dependence of the conductance is predicted a priori remarkably well, assuming a generic value of 4.7 for the intrinsic pK_a of the isolated carboxyl group (smooth curve of Figure 3). The low- and high-pH asymptotes indicate a 4-fold difference in conductance between the fully protonated and fully deprotonated forms of the channel. Mapped onto the conductance−concentration curve for wild-type KcsA (*7*), this increased conductance corresponds to an ~8-fold enhancement of local K^+ concentration (inset in Figure 3, dashed lines), equivalent to a potential of −54 mV imposed by the four fully charged side chains. In this analysis, we deliberately focus on the chord conductance measured at voltages sufficiently positive so that the measured current reflects solely the unidirectional outward flux of K^+, uncontaminated by inward flux, but not so high that diffusion limitation sets in; as discussed previously (*10*), we find 100−200 mV to be an optimal range of voltage for this purpose.

Does this electrostatic maneuver played out on a KcsA channel have any relevance to the exceptional conductance of BK-type channels? To find out, we compared a mammalian BK channel, mSlo (*9*), with a mutant in which both of the glutamates highlighted in Figure 1c were neutralized (E321N/E324N). These neutralized channels are indeed smaller than wild type, but by only a factor of ~2 (Figure

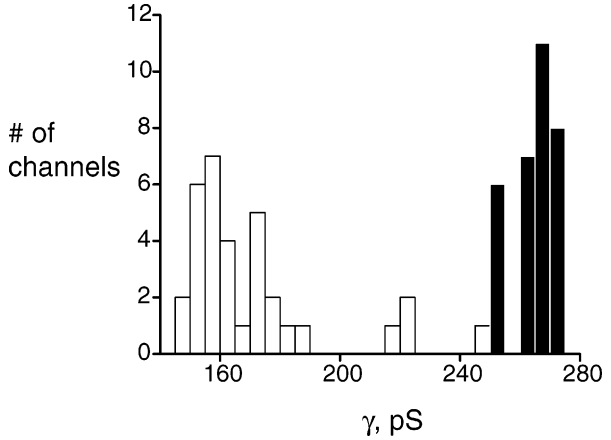

FIGURE 5: Distribution of BK conductance values. Single-channel recordings were collected from oocytes injected with wild type or mutant RNA. Conductances between 0 and 100 mV were histogramed for 32 wild-type (black bars) and 33 E321N/E324N mutant (white bars) channels. The four channels with conductance values between 220 and 250 pS for the mutant-injected oocytes were omitted from averaging in the $I-V$ curve shown in Figure 4c.

4). As expected from the sided nature of the charge alteration (*17*), the reduction in conductance is most prominent at positive voltages, though still apparent throughout the voltage range (Figure 4c). To the extent that the BK channel structure resembles that of MthK, this result suggests that an electrostatic mechanism may be at work here as well.

We note as a peripheral issue that the double mutant BK channels show more variation in single-channel conductance than wild type, as seen in histograms of single-channel conductance values from our full set of patches (Figure 5). Most channels recorded from mutant-injected oocytes cluster around an average conductance of 160 pS, but a minor fraction of channels are larger than the main population, close in value to the wild-type conductance. These larger channels may represent endogenous oocyte BK channels or heteromers of mutant and endogenous channel subunits. However, the possibility of subunit mixing means that the true conductance of a homomeric mutant tetramer is, if anything, lower than the observed conductance and that the true impact of the mutation is, if anything, greater than what we report.

In summary, we have shown that introduction of negative charges at the intracellular entryway of KcsA increases the unitary conductance 4-fold, into a range characteristic of BK channels. Moreover, the quantitative utility of a simple multiple-protonation treatment argues strongly for a through-space electrostatic mechanism underlying this conductance increase. We have also shown, conversely, that neutralization of conserved negative charges in the same region of a BK channel results in a decrease in conductance, but only ~2-fold, still well above conductances of most K^+ channels. Therefore, the high conductances of BK-like channels can be only partly attributed to vestibule electrostatics. Is this because the MthK structure is not an adequate model for the BK channels? If not, where do the differences lie—in structural subtleties of the selectivity filter or gross differences in vestibule architecture? Alternatively, is it possible that the crude Coulombic theory employed here is only adventitiously successful for KcsA but must be expanded to a full Poisson−Boltzmann treatment for a general application to both channels? These questions are currently unanswerable, but an alternative conjecture for the difference in electrostatic responsiveness of KcsA and BK emerges naturally from considering each channel's $\gamma-[K^+]$ relation (Figures 3 and 4c). This function is "flatter" for the BK channel than for KcsA (*17*), and so the BK conductance should be less sensitive to a decrease of local $[K^+]$ upon removing charge than KcsA is to introducing the same charge. In the absence of a full $\gamma-[K^+]$ relation for the mutated BK channel in a biochemically defined system, this suggestion must remain only qualitative. Nonetheless, the results here show that an effective and evolutionarily feasible strategy for modulating a channel's absolute conductance is to embroider charges on the fabric of its ion entryway.

ACKNOWLEDGMENT

We are grateful to C. Williams and L. Kolmakova-Partensky for construction of mutants, to Dr. Dan Cox for *Xenopus* therapy, and to Dr. Karl Magleby for the BK channel clone. We thank Drs. Lise Heginbotham and Steve Goldstein for sharing results on KcsA mutants before publication.

REFERENCES

1. Heginbotham, L., Lu, Z., Abramson, T., and MacKinnon, R. (1994) *Biophys. J. 66*, 1061−1067.
2. Doyle, D. A., Cabral, J. M., Pfuetzner, A., Kuo, J. M., Gulbis, J. M., Cohen, S. L., Chait, B. T., and MacKinnon, R. (1998) *Science 280*, 69−76.
3. Jiang, Y., Lee, A., Chen, J., Cadene, M., Chait, B. T., and MacKinnon, R. (2002) *Nature 417*, 523−526.
4. Jiang, Y., Lee, A., Chen, J., Ruta, V., Cadene, M., Chait, B. T., and MacKinnon, R. (2003) *Nature 423*, 33−41.
5. Hille, B. (2001) *Ion Channels of Excitable Membranes*, 3rd ed., Sinauer Associates, Sunderland, MA.
6. Latorre, R., Oberhauser, A., Labarca, P., and Alvarez, O. (1989) *Annu. Rev. Physiol. 51*, 385−399.
7. LeMasurier, M., Heginbotham, L., and Miller, C. (2001) *J. Gen. Physiol. 118*, 303−314.
8. Heginbotham, L., Kolmakova-Partensky, L., and Miller, C. (1998) *J. Gen. Physiol. 111*, 741−750.
9. Butler, A., Tsunoda, S., McCobb, D. P., Wei, A., and Salkoff, L. (1993) *Science 261*, 221−224.
10. Nimigean, C. M., and Miller, C. (2002) *J. Gen. Physiol. 120*, 323−335.
11. Yellen, G. (2002) *Nature 419*, 35−42.
12. Jiang, Y., Lee, A., Chen, J., Cadene, M., Chait, B. T., and MacKinnon, R.(2002) *Nature 417*, 515−522.
13. del Camino, D., and Yellen, G. (2001) *Neuron 32*, 649−656.
14. Heginbotham, L., LeMasurier, M., Kolmakova-Partensky, L., and Miller, C. (1999) *J. Gen. Physiol. 114*, 551−560.
15. Irizarry, S. N., Kutluay, E., Drews, G., Hart, S. J., and Heginbotham, L. (2002) *Biochemistry 41*, 13653−13662.
16. Wyman, J., and Gill, S. J. (1990) *Binding and Linkage*, 330 pp, University Science Books, Mill Valley, CA.
17. MacKinnon, R., Latorre, R., and Miller, C. (1989) *Biochemistry 28*, 8092−8099.

BI0348720